Flexible Generation of Equivalent Beams for Digital Beamforming SAR Systems with Different Antenna Structures

Sebastian Bertl[(1)], Paco López-Dekker[(1)], Marwan Younis[(1)], Gerhard Krieger[(1)]

[1] *German Aerospace Center, Mircowave and Radar Institute*
Oberpfaffenhofen, Germany

INTRODUCTION

Digital beamforming is known to open new options in improving the performance of potential future SAR systems in terms of sensitivity and ambiguity suppression. In addition, digitally available channels also increase the measurement flexibility of certain hardware setups by opening up the possibilities to realise specific requirements using different technologies. It is briefly shown with data from experiments using the TerraSAR-X satellite that digital beamforming offers the possibility of combining channels to form new beams and can also be used to transform squnited beams into beams with different phase centres. A possible application that will be addressed in the following is the realisation of a system for along-track interferometry or GMTI. An application driven design approach would lead to a planar array solution with several channels in along-track direction. Yet at higher frequencies, like at Ka-band, sensitivity requirements connected with hardware properties lead to the conclusion that a setup using a reflector antenna can provide better performance than a planar array. The conflict in choice of antenna setups for a realisation of along-track interferometry can be overcome by exploiting the flexibility offered by a SAR system with digitally available channels.

EXPERIMENTAL DEMONSTRATION OF DIGITAL BEAMFORMING AND EQUIVALENT BEAMS

An experiment, initially intended to demonstrate digital beamforming, can be used to further demonstrate the equivalency of different sets of digital beams as they would come from different antenna configurations sampled digitally such as planar arrays and reflector antennas.

In a similar way as TerraSAR's Dual-Receive antenna [1] in along-track direction, beams with different phase centres can also be generated in elevation, but by attenuating parts of the phased array antenna on receive. An experiment described in [2] can provide data acquired in this antenna configuration. In addition, images from the same area on ground were acquired using two narrower beams with different main beam directions on receive as they could be generated directly from a reflector antenna using only specific feeds on receive. The two sets of beams are shown in Fig. 1a and 1b with amplitude and phase.

To show that the two sets of beams are initially acquiring data in different ways, but still can be considered equivalent, the transformation

$$\begin{bmatrix} a_1' \\ a_2' \end{bmatrix} = 0.5 \cdot \begin{bmatrix} \exp(j \cdot \pi/2) & \exp(j \cdot 0) \\ \exp(j \cdot 0) & \exp(j \cdot \pi/2) \end{bmatrix} \cdot \begin{bmatrix} a_1 \\ a_2 \end{bmatrix}, \tag{1}$$

with the complex antenna patterns $\{a_i, a_i' \in \mathbb{C}\}$, can be used to change the two beams with different look directions but same phase centre into two beams with same beamwidth as if they would come from narrower antenna segments but with different phase centres. The generated beams are shown in Fig. 1c with amplitude and phase. As input the patterns shown in Fig. 1a are used. The resulting beams correspond to the beams of Fig. 1b as the dashed lines in Fig. 1c illustrate.

The SAR processed data are shown in Fig. 2 for the three different sets of beams: the two original sets and the result of the transformation according to (1). For each set the first two pictures show the reconstruction result when only one beam is used. The third picture is the interferometric phase of the two SAR images.

Since the results in Fig. 2 a are from a pair of beams that have the same phase centre but are looking in different directions, the amplitude images show different intensities in near and far range. The interferometric phase is zero, as shown by the uniform turquoise colour.

The second group of images shown in Fig. 2 b is acquired with the beams shown in Fig. 1b. The acquisition was performed 3 months after the first one, such that the river shows a change related to having more water. The amplitude images look the same, since the beams have the same shape. The phase of the interferogram shows now a change from near to far range due to the different phase centres of the two beams.

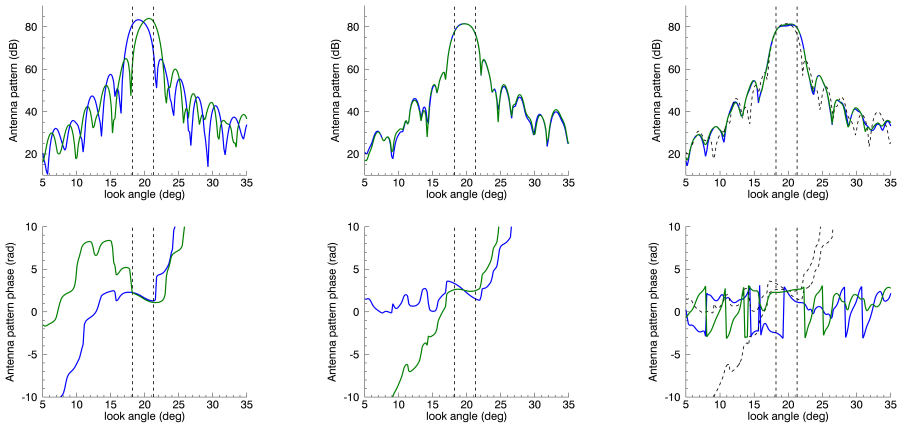

(a) Set of beams with different elevation direction of the main lobe

(b) Set of beams with different phase centres in elevation but same pattern

(c) Beams generated from beams of Fig. 3a using (1). Dashed lines show beams from Fig 3b

Fig. 1: Overview over the two sets of realised beams for TSX and the transformed antenna patterns

Using the transformation (1), the beams shown in Fig. 1a can be transferred into the beams shown in Fig. 1c. The amplitude in the SAR images is now more uniform than it is the case for using the original beams. In addition, the phase of the interferogram is now showing almost the same transition from near to far range as with the second set of beams (cf. Fig. 2 c). Both the antenna pattern and the resulting image show that the first set of beams and its resulting SAR image are equivalent to the second set of beams after using the transformation in (1).

FORMATION OF MULTIPLE PHASE CENTRES ON A REFLECTOR ANTENNA WITH A DIGITAL FEED ARRAY

Reflector antennas are considered in the last years for the application in spaceborne SAR systems. Typically the systems would be equipped with a reflector antenna and a feed array with several feed elements. The signals of the feed elements are available for further processing as they are digitised individually. The considered reflector antennas have a parabolic curvature and in general the array of feed elements is centred around the focal point of the reflector.

In the following, it is considered that the feed array is extended along azimuth direction with several elements. The activation of a single feed element will generate a narrow beam in a certain direction, as illustrated in Fig. 3a. Each feed will generate a beam looking into a different direction, acquiring a different part of the Doppler band.

When all feeds of a reflector are activated simultaneously, as shown in Fig. 3b, a narrower beam to illuminate the reflector will be generated. By calibrating the transmit and receive modules, the fields of the different feeds are in phase and constructively generate the incident field on the reflector surface. The larger azimuthal extension of the feed array compared to a single feed element will have the consequence that only a part of the reflector is getting illuminated, which results in a wider far-field beam.

By shifting the centre of the surface currents on a reflector, the phase centre can be shifted. Shifting of the surface currents is done by activating several feed elements to generate a narrow beam, that does not cover the complete reflector, and by additionally applying a phase term $\phi(n)$ that changes linearly with the position of the feed elements according to

$$\phi(n) = \frac{2\pi}{\lambda} \cdot \Delta x_{\text{feed}} \cdot \sin(\theta) \cdot n, \qquad n = 0, \ldots, N-1, \tag{2}$$

with Δx_{feed} being the spacing between the elements, θ the steering angle of the primary beam that generates the surface currents and n the index of the specific feed element. This concept, which is commonly applied to phased arrays, can be utilized in both transmit and receive case. The number of independent phase centres

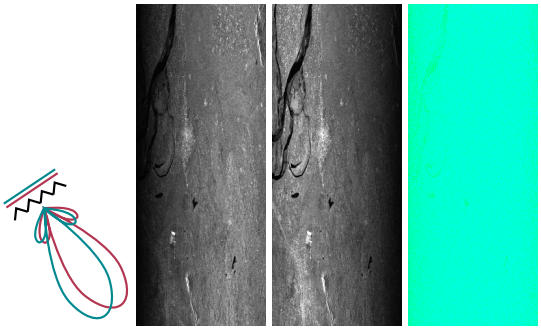

(a) Results for squinted beams, same phase centre, see Fig. 1a

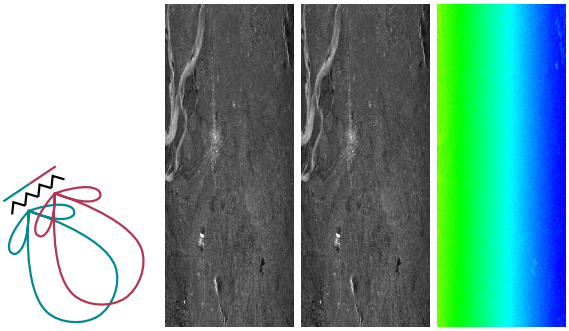

(b) Results for beams with different phase centres, see Fig. 1b

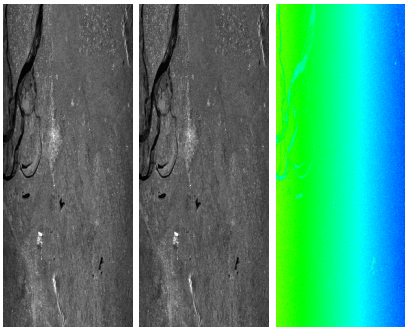

(c) Results for transformed beams, see Fig. 1c

Fig. 2: Different reconstruction results showing the equivalent results after transformation of squinted beams to a case with different phase centres

that can be generated simultaneously to receive signals is equal to the number of feed elements. The described concept is illustrated in Fig. 3c. Each far field beam will be generated by surface currents that occupy only a narrow part on the reflector. The resulting beams will be wider than the beam of a single element. All beams will look in the same direction, but their phase centres are at different positions. With these properties the beams, originating from a digital feed array and a single reflector, can therefore be used for along-track interferometry.

In addition to the positioning capability, the amount of phase centres can be controlled depending on the amount of feed elements in the array. The size of the apertures of each phase centre can be adjusted as well. The probably most essential feature in terms of a later application is, that this concept can be implemented on any system with a large reflector antenna and a digital feed array, that is designed as a conventional DBF-SAR that could work according to the high resolution wide swath concept (HRWS). Currently considered systems

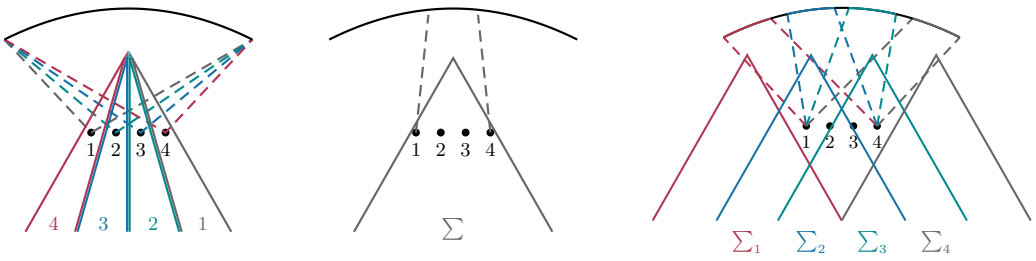

(a) Activation of single feed elements

(b) Simultaneous activation of all feed elements in phase

(c) Simultaneous activation of all feed elements with linear phase offset between elements

Fig. 3: Illustration of beams resulting from different activation of azimuth feed elements

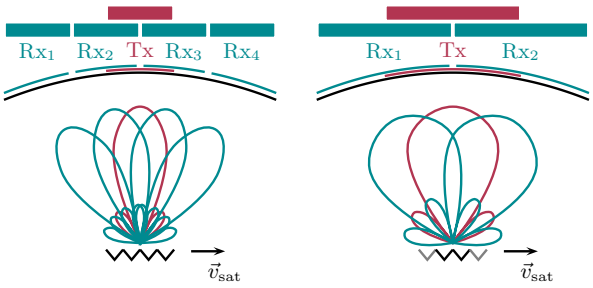

(a) Four smaller Rx phase centres (green) and one Tx phase centre, with wider far field beams

(b) Two phase centres on receive, one on transmit (only two feeds active)

Fig. 4: Schematic illustration of a setup with a single reflector antenna that can be used for ATI-SAR in different modes regarding size, position and amount of phase centres and therefore receive channels

for future missions do not need any hardware adaption in order to use it for interferometry as described in the following. This makes the described approach very appealing for current system studies. An existing airborne system that already shows all the required properties is the Ka-band SweepSAR system [3].

KA-BAND SYSTEM SUGGESTION AND ITS INITIAL SAR PERFORMANCE

The implementation of along-track interferometry with a single reflector antenna is especially interesting at higher frequencies, e. g. Ka-band, since the required along-track baselines for applications like the measurement of ocean currents or land traffic monitoring, are in the order of few meters and could be implemented efficiently on a single platform. At Ka-band, system studies show that losses in transmission lines and switching networks are high. The design of an efficient system using direct radiating arrays is difficult, when baselines of several meters should be generated. The benefit of a reflector-based antenna setup would be that it keeps the feed array and its RF network compact and close to the satellite body as it would be desirable in terms of low system losses. Planned missions using Ka-band frequencies as the SWOT mission [4] and current studies [5] are based on structures that span physical baselines of 10. . . 20 m. In the case of the SWOT mission a reflectarray with 5 m length is used. Similar antenna dimensions are of interest for ATI in the current context.

A possible schematic antenna setup that exploits the concept of along-track interferometry using a single reflector antenna is shown in Fig. 4. The schematic setup shows one large reflector that is illuminated by a feed array placed in the focal point of the reflector. The system can be operated in different configurations, in order to adapt amount and size of the phase centres to different scenarios. The setup can be changed during flight depending on the desired application.

Due to the small wavelength of 8.4 mm, the mechanical and thermal stability needs to be addressed, especially when structures spanning several metres are required. For architectures with large booms of up to 10 m as in [5], metrological instruments placed close to the feed array are considered to measure the oscillations and thermal distortions of the reflectors placed on the tip of the boom.

Regarding the interferometric baseline, a characterisation of the antenna on ground for different supplied phase terms as in (2) on the digital feed array can provide a first calibration. However due to the mentioned thermal and mechanical distortions, relevant changes in terms of baseline variation need to be addressed in addition. For a calibration during flight the coregistration of the images to the different phase centres of a fixed target above land can provide a way to constantly calibrate the along-track baseline.

As a first study, a parabolic reflector with a width of 8 m and a feed array consisting of five elements is considered. A summary of parameters is given in Tab. 1. In Fig. 5 four different realisations of surface currents on the reflector surface are shown. The surface currents are located at different areas of the reflector surface, which corresponds to four different phase centres. Without knowledge of the surface currents, a calibration over a fixed target above land can be considered. This approach is demonstrated in Fig. 6 b. The phase difference of the far fields of different phase centres is evaluated. Due to the different phase centre positions a phase difference in the far field patterns over the look angle occurs. In the main lobe region this phase change is almost linear

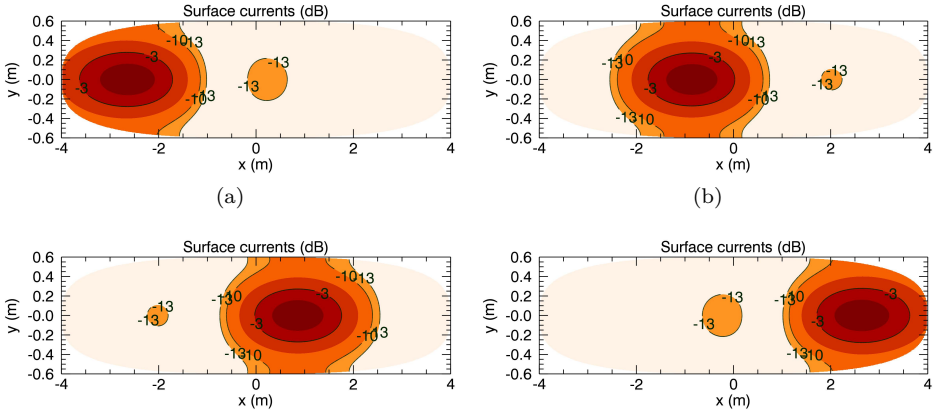

Fig. 5: Surface currents on the parabolic reflector for different phase shifts applied to the feed array elements according to (2)

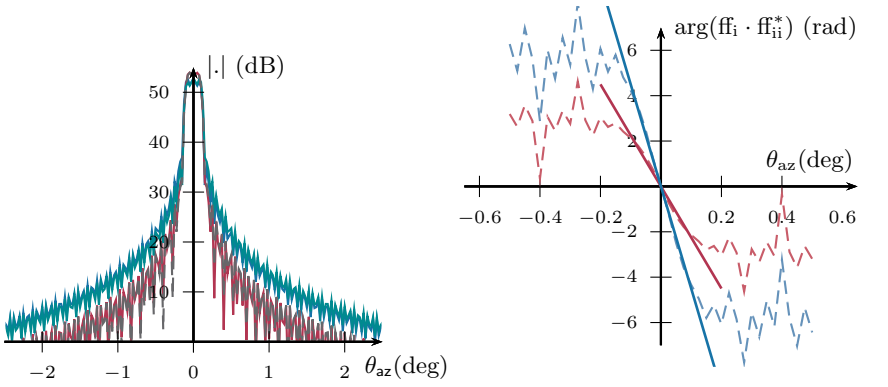

(a) Far field plots

(b) Phase difference of two pairs of far-field pattern, middle two in red and middle and outer phase centre in blue

Fig. 6: Far-field properties of the four generated phase centres as in Fig. 5

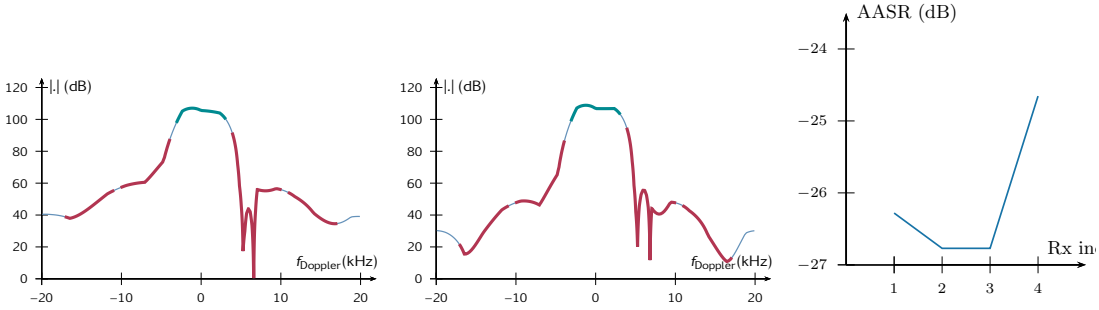

(a) Signal and ambiguity Doppler bands for Rx 1

(b) Signal and ambiguity Doppler bands for Rx 2

(c) Azimuth ambiguity to signal ratio at 31° look angle

Fig. 7: Azimuth performance of the four Rx channels

Tab. 1: Parameters of the considered Ka-band ATI system

Parameter	Value
Centre frequency	35.5 GHz
Reflector width	8 m
Reflector height	1.2 m
Focal length	8 m
Feed elements	5
Feed dimension (width, height)	$(0.8, 14)\,\lambda$
Pulse repetition frequency	7000 Hz

and is related to the separation B of the phase centres through

$$B = \frac{\lambda}{2\pi} \cdot \frac{\Delta\Phi}{\Delta\theta_{\mathrm{az}}}, \tag{3}$$

where $\Delta\Phi$ is the phase change along the angular interval $\Delta\theta_{\mathrm{az}}$ and λ the wavelength.

Evaluating the linear slope in Fig. 6 b results in distances between different phase centres. Two distances can be derived, one from an inner phase centre to the other inner phase centre (Fig. 5 b and c) as $B_{\mathrm{centre,\,centre}} = 1.70\,\mathrm{m}$ and the other from an inner phase centre to an outer one (Fig. 5 b and d) with $B_{\mathrm{centre,\,side}} = 3.41\,\mathrm{m}$. These two relative distances correspond to positions of the phase centres along azimuth at the positions $x_{\mathrm{az}} = \pm 0.85\,\mathrm{m}, \pm 2.56\,\mathrm{m}$, such that according to Fig. 4 a the positions of the phase centres would be $x_{\mathrm{Rx}_1} = -2.56\,\mathrm{m}$, $x_{\mathrm{Rx}_2} = -0.85\,\mathrm{m}$, $x_{\mathrm{Rx}_3} = 0.85\,\mathrm{m}$ and $x_{\mathrm{Rx}_4} = 2.56\,\mathrm{m}$. These positions calculated using the linear slope in Fig. 6 b also resemble the positions of the maximum surface currents in the four plots in Fig. 5. To show that the four phase centres show similar performance among each other in a SAR application, the azimuth ambiguity to signal ratio (AASR) is calculated. The Doppler band and the four closest ambiguity bands for a phase centre at the edge and a phase centre in the centre of the reflector antenna is shown in Fig. 7 a and b. The AASR value for all four phase centres at a look angle of 31° is plotted in Fig. 7 c. Along range the ambiguity suppression will mainly depend on the amount of feed elements that are available for digital beamforming (SCORE).

CONCLUSION

Digital beamforming offers in addition to improved SAR performance also an increased flexibilty in implementing different operational modes with the same hardware. Beams of single receive elements can be combined in a processing step to generate new sets of beams with different properties. As an experimental demonstration beams acquired with TSX in two different ways were transformed into each other and show the same properties. An interesting application of this fact lies in the along-track interferometry with several closely spaced phase centres at higher frequencies, such as Ka-band. A single reflector antenna can be used to generate an along-track interferometric measurement setup, while exploiting all the benefits of a reflector antenna, mainly the low losses due to compact TR modules compared to setups with distributed phased array antennas.

References

[1] M. Gabele, B. Brautigam, D. Schulze, U. Steinbrecher, N. Tous-Ramon, and M. Younis, "Fore and aft channel reconstruction in the TerraSAR-x dual receive antenna mode," *IEEE Transactions on Geoscience and Remote Sensing*, vol. 48, no. 2, pp. 795–806, 2010.

[2] S. Bertl, P. Lopez-Dekker, S. Wollstadt, and G. Krieger, "Demonstration of digital beamforming in elevation for spaceborne synthetic aperture radar," in *2014 10th European Conference on Synthetic Aperture Radar (EUSAR)*, 2014, abstract submitted.

[3] G. A. Sadowy, H. Ghaemi, and S. C. Hensley, "First results from an airborne ka-band SAR using SweepSAR and digital beamforming," in *9th European Conference on Synthetic Aperture Radar, 2012. EUSAR*, Apr. 2012, pp. 3–6.

[4] G. Dibarboure, S. Labroue, M. Ablain, R. Fjortoft, A. Mallet, J. Lambin, and J.-C. Souyris, "Empirical cross-calibration of coherent SWOT errors using external references and the altimetry constellation," *IEEE Transactions on Geoscience and Remote Sensing*, vol. 50, no. 6, pp. 2325–2344, Jun. 2012.

[5] C. Schaefer, M. Völker, P. Lopez-Dekker, M. Younis, E. Daganzo-Eusebio, and M. Ludwig, "Space-borne ka-band across-track SAR interferometer," in *Proceedings 1st KEO Workshop*, Noordwijk, The Netherlands, 2012, pp. 1–8.